Thermodynamic Structural and Morphological Investigation of Poly(Vinylidene Fluoride)−Camphor Systems, Preparing Porous Gels from a Solid Solvent

D. Dasgupta,[†] S. Manna,[†] S. Malik,[‡] C. Rochas,[§] J. M. Guenet,*[,‡] and A. K. Nandi*[,†]

Polymer Science Unit, Indian Association for the Cultivation of Science, Jadavpur, Kolkata 700032, India, Institut Charles Sadron, CNRS UPR 22, BP 40016, 6 Rue Boussingault, 67083 Strasbourg Cedex, France, and Laboratoire de Spectrometrie Physique CNRS-UJF UMR5588, 38402 Saint Martin d'Heres Cedex, France

Received March 19, 2005; Revised Manuscript Received May 9, 2005

ABSTRACT: Poly(vinylidene fluoride) (PVF_2)−camphor systems have been investigated in concentrations ranging from $W_{PVF2} = 0$ to 1 (w/w). The temperature−concentration phase diagram suggests the formation of two different polymer−solvent compounds of an incongruently melting type (C_1 and C_2), a eutectic transition, and a metatectic transition. The data related to the melting enthalpy of the different first-order events provide one with stoichiometries of 1/2 and 1/4 for compound C_1 and compound C_2, respectively (number of camphor molecules per PVF_2 monomer). Time-resolved X-ray experiments carried out as a function of temperature also support the existence of two different compounds. The optical microscopy shows an abrupt change of texture with increasing temperature. The morphology as observed from SEM after drying under vacuum shows tubular, porous structures for concentration below the stoichiometric composition of compound C_2 and the appearance of spherulites above.

Introduction

Thermoreversible polymer gels have been studied extensively for the past two decades,[1−3] as they are interesting candidates for preparing porous membranes, or more generally, randomly dispersed structures. Poly(vinylidene fluoride) (PVF_2), a technologically important polymer,[4] produces thermoreversible gels in different solvents containing ⟩C═O group.[5−7] Extensive studies of the physical properties of the PVF_2 gels have been carried out for diesters of varying intermittent length.[7] The thermoreversible PVF_2 gels possess a three-dimensional network structure made up from an array of fibrils, which eventually produces a porous structure once the solvent is removed. By increasing the number of intermittent carbon atoms, fibrils become finer.[7] Retaining this network structure intact is important once the gel has been dried. However, drying of these gels prepared from solvents that are liquid at room temperature, while keeping the network structure virtually intact to produce porous material,[8] is a difficult task, especially when no freeze-drying procedure can be brought about. This is the reason we have focused our attention onto camphor, a solid at room temperature, which sublimates easily and can thus be removed readily by simply applying vacuum.

Camphor is a bicyclic compound (1,7,7-trimethyl bicyclo[2,2,1] heptane-2-one) containing a ⟩C═O group. As a result, there is a possibility of interaction between the ⟩C═O group and ⟩CF_2 dipole of PVF_2, [9,10] and so the later may be soluble in camphor in the liquid state, but also, as with diesters, to form complexes with this polymer. Further, PVF_2 crystallizes in five different polymorphs: α, β, γ, δ, and ϵ, of which α is the commonest polymorph where the chain takes on a $TGT\bar{G}$ conformation. Whether camphor has any influence to produce a particular polymorph of PVF_2 will also be of interest.

The formation of gel structure in the solid state is not uncommon as it has been reported previously in polyaniline−surfactant and PVF_2−surfactant gels.[11−13] It produces an elastic mass arising from the network structure[12] and also exhibits reversible first-order phase transition.[11,13] However, with increasing polymer concentration, gel structure may be lost.[11] The gel structure is accompanied by polymer−solvent compound formation in PVF_2−diester gels,[7,14] and in the PVF_2−camphor gel, such polymer−solvent complexes may also be produced. The polymer−solvent complexation is usually determined from thermodynamic, X-ray, and spectroscopic investigations.[7,15,16] In this paper, we present results on how camphor affects the structure, thermodynamics, and morphology of PVF_2. The temperature−concentration phase diagram is established, the morphology is observed, and the outcomes are examined in light of time-resolved X-ray experiments (synchrotron radiation). Molecular structures are tentatively put forward by using a molecular mechanics (MMX) program.[17]

Experimental Section

Samples. Poly(vinylidene fluoride) (PVF_2) is a product of Aldrich Chemical Co. Inc. The weight-average molecular weight ($\bar{M}_w$) of the sample is 1.8×10^5, and the polydispersity index is 2.54, as obtained from GPC. The PVF_2 sample was recrystallized from its 0.2% (w/w) solution in acetophenone. DL-Camphor (S. D. Fine Chem. Ltd., Mumbai) was purified by a sublimation procedure in a vacuum at 50 °C.[18]

Sample Preparation and Characterization. The PVF_2 and camphor were taken in a thick walled glass tube (8 mm in diameter and 1 mm thick) and were sealed. The sealed tubes were melted at 210 °C in an oven for 20 min with intermittent shaking to make homogeneous. They were then quenched to

* Authors to whom correspondence should be addressed. E-Mail: psuakn@mahendra.iacs.res.in (A.K.N.); guenet@ics.u-strasbg.fr (J.M.G.).
[†] Indian Association for the Cultivation of Science.
[‡] Institut Charles Sadron.
[§] Laboratoire de Spectrometrie Physique.

10.1021/ma050582a CCC: $30.25
Published on Web 06/03/2005

30 °C. For SEM study, the samples were taken out from the tube and kept in a vacuum for 2 days to remove the camphor. It was then gold coated with a gold layer of thickness 40 nm by the sputtering technique in an argon atmosphere and was then observed in a SEM apparatus (Hitachi S-2300). The FT-IR study was done using a Nicolet FT-IR instrument (Magna IR 750 spectrometer, Series II) using the PVF_2−camphor gel. The gel spectrum was then subtracted from the camphor spectrum to obtain the PVF_2 spectra in the gel state.

Thermal Characterization. For thermodynamic study, the gels were prepared in Perkin-Elmer large volume capsules (LVC) by taking an appropriate amount of polymer, and the camphor and the capsules were tightly sealed with help of a quick press. They were subsequently made homogeneous by keeping the samples at 200 °C in a DSC (Perkin-Elmer DSC-7) for 15 min with occasional shaking and gelled at 50 °C for 10 min by cooling from 200 °C at the rate of 200 °C/min. They were then heated with a scan rate of 40°/min twice to 200 °C under nitrogen atmosphere to make homogeneous. Finally, they were heated at the scan rate of 2 °C/min under nitrogen atmosphere from 50 to 200 °C. The enthalpy(s) and melting temperature(s) were measured using a computer attached to the instrument. Cooling runs were also taken from the melt at 200−50 °C at the rate of 5 °C/min. The instrument was calibrated with indium before each set of experiments.

WAXS Investigation. The WAXS experiments were carried out on two types of samples (i) as-prepared and (ii) after vacuum-drying at room temperature. The later experiments were performed in a Seifert X-ray diffractometer (C3000) with nickel-filtered copper K_α radiation equipped with a parallel beam optics attachment. The instrument was operated at a 35 KV voltage and at 30 mA current, and was calibrated with standard silicon sample. The samples were scanned from a $2\theta = 2°$ value at the step scan mode (step size 0.03°, preset time 2 s,) and the diffraction pattern was recorded using a scintillation counter detector.

The temperature variation X-ray experiments in the gel state were carried out on beamline BM2 at the European Synchrotron Radiation Facility (ESRF), Grenoble, France. The energy of the beam was 15.8 KeV, which corresponds to a wavelength of $\lambda = 7.86 \times 10^{-2}$ nm. At the sample position, the collimated beam was focused with a typical cross section of 0.1×0.3 mm^2. The scattered photons were collected onto a two-dimensional CCD detector developed by Princeton Instruments, presently Roper Scientific. Typical acquisition times are of about 10−20 s, which allows time-resolved experiments to be carried out at 2 °C/min, a value similar to the heating rate used for DSC experiments.

The sample-to-detector distance was about 0.2 m, corresponding to a momentum transfer vector q range of $1 < q$ (nm^{-1}) < 17, with $q = (4\pi/\lambda)\sin(\theta/2)$, where λ and θ are the wavelength and the scattering angle, respectively (further information are available on the following website http://www.esrf.fr). The scattering intensities obtained were corrected for the detector response, the dark current, the empty cell, the sample transmission, and the sample thickness. To obtain a one-dimensional X-ray pattern out of the two-dimensional digitalized pictures, the data were radially regrouped, and a silver behenate sample was used for determining the actual values of the momenta transfer q.

Samples were prepared in thin-walled glass tubes of 3 mm inner diameter and 5 cm high that were hermetically sealed from atmosphere to prevent evaporation during temperature scan. A minimum of 200 mg of material was used to make sure that the sample was homogeneous throughout. This aspect of sample preparation is of importance as the diffraction pattern can be highly dependent upon the solvent content when polymer−solvent compounds are dealt with. Inhomogeneous samples can then give off confusing diffraction patterns. The higher concentrations were prepared from low-concentrated samples by evaporating camphor, sealing the glass tube, and heating again above the melting point of the mixture until a homogeneous solution was produced, and then cooling to room temperature.

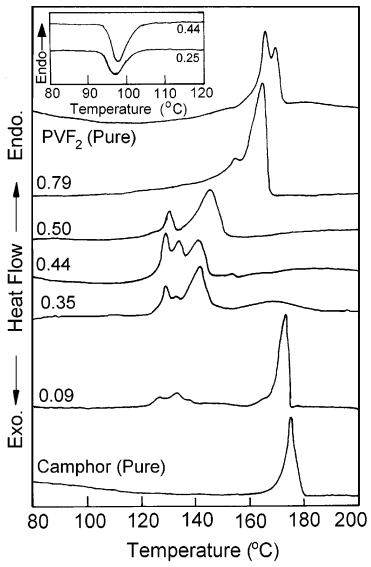

Figure 1. DSC thermograms of PVF_2−camphor system at indicated weight fraction of PVF_2. The samples were melted at 200 °C twice and then quenched to 50 °C. It was then heated at the rate of 2°/min. (Inset: cooling thermogram from melt at 200 °C at the cooling rate of 5°/min].

Optical Microscopy. The samples used for optical observation were prepared by remelting between glass slides those samples prepared beforehand in a test tube. To minimize solvent evaporation, the edge of the thin upper glass slide was glued with epoxy resin. A Mettler FP82HT hot stage operated by an FP90 central processor was used, which allowed observation of the different morphological transformations taking place on heating at a rate of 2°C/min. The phase contrast optical investigations were carried out with a NIKON Optiphot-2 equipped with a CCD camera and using LUCIA a software developed by Laboratory Imaging for image processing and analysis.

Molecular Modeling. Approximate molecular models of polymer−solvent (PVF_2−camphor) complexes are obtained from a personal computer (Pentium III) using a molecular mechanics (MMX) program.[7,17] The structure of α-polymorph PVF_2 and that of camphor molecules are drawn with the help of the program, such that the oxygen atom of a ⟩C═O group of camphor faces the carbon atom of the ⟩CF_2 group of PVF_2. The whole structure was then energetically minimized with the help of the MMX program in the computer. The distances between the carbon atom of ⟩CF_2 group and the oxygen atom of the ⟩C═O group were queried and also that between the two PVF_2 strands of the complex from the program. The experiment was done for different compositions of the polymer solvent complexes discussed below.

Results and Discussion

Thermodynamics: Phase Diagrams. Typical differential scanning calorimetry (DSC) thermograms of PVF_2−camphor systems obtained at 2°C/min are shown in Figure 1 for different polymer fractions corresponding to salient thermal events. Also, the thermoreversible nature of this system is clarified from the cooling thermograms at the inset of the figure. Essentially, three typical types of behavior are seen: for polymer fractions below $W_{PVF2} = 0.44$, one can observe four endotherms; above this polymer fraction, three endotherms are seen up to $W_{PVF2} = 0.59$ and two endotherms for the remaining compositions. The existence of two endotherms for pure PVF_2 arises from the occurrence of lamellar thickening,[19,20] the first endotherm corresponding to the transformation of thin lamellae into thicker ones. For establishing the tem-

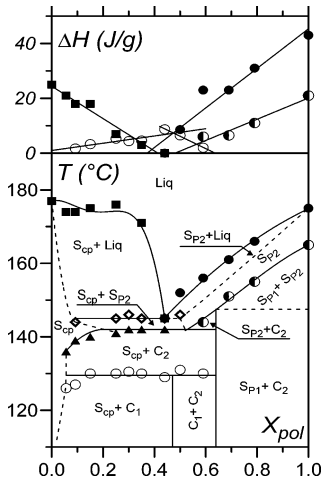

Figure 2. *Top*: Tamman's diagrams of PVF_2–camphor system: ■ enthalpy of camphor melting, ○ enthalpy of lowest melting peak, ◐ enthalpy of melting corresponding to Sp_1, and ● enthalpy of melting corresponding to Sp_2 (all are deconvoluted). *Bottom*: Phase diagram of PVF_2–camphor system. S_{cp} = solid solution of camphor and PVF_2, C_1 = polymer–solvent compound 1, C_2 = polymer–solvent compound 2, Sp_1 = PVF_2 solid (unthickened) and camphor mixture, Sp_2 = PVF_2 solid (thickened) and camphor mixture.

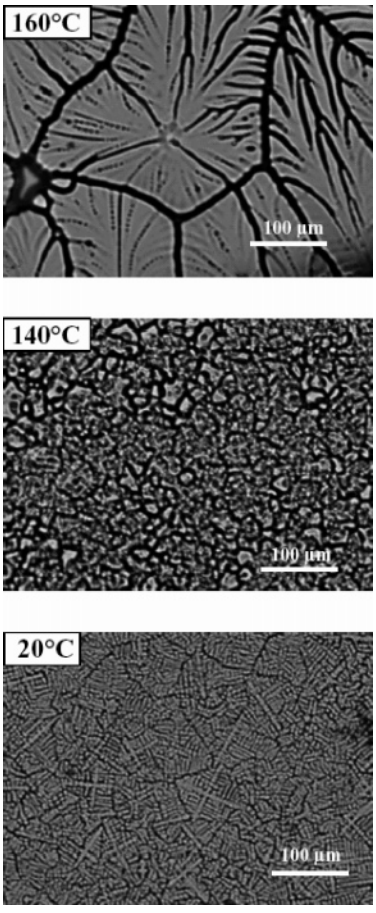

Figure 3. Optical micrographs of PVF_2–camphor system (W_{PVF2} = 0.15) at indicated temperatures.

perature–concentration phase diagram (namely, melting and/or transition temperature vs polymer concentration), the maxima of the endotherms were taken. For establishing the Tamman's diagram (namely, melting and/or transition enthalpies vs polymer concentration), a deconvolution procedure was used for calculating the

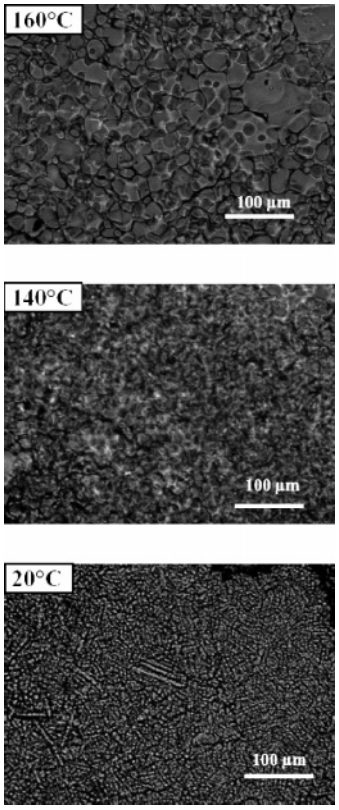

Figure 4. Optical micrographs of PVF_2–camphor system (W_{PVF2} = 0.60) at indicated temperatures.

enthalpies associated with each endotherm, especially for systems exhibiting four endotherms. The values of the different enthalpies were obtained from several runs with the same sample. In the case where four or three endotherms were observed, the value of the enthalpy associated with the first and the last endotherms were definitely reproducible, yet it was not so with the enthalpies of the other two (or one) intermediate endotherm(s). While the sum of these intermediate endotherms was a constant within experimental uncertainties, a large variation for the enthalpy of each endotherm was observed. This certainly arises from the deconvolution procedure, which is carried out without a clear knowledge of the shape of each endotherms. As a result, we have decided not to give these values on the Tamman's diagram[15] to avoid confusion.

These results are summarized in Figure 2, where the temperature–concentration phase diagram together with the Tamman's diagram are drawn. As can be seen, three nonvariant events occur at T = 130, 142, and 145 °C. Phase rules edicted by Gibbs, particularly that dealing with the value of the variance of a two-constituent system, and that of the lever rule which provides one with the fraction of each phases, have been applied (further reading on these rules can be found in ref 2 with references therein). As is customary, the probable, yet not explicitly observed, extensions of the different domains are delimited with dotted lines. It is worth emphasizing that these extensions are plausible but may not be unique. The following outcomes are deduced from this phase diagram:

(i) There probably exist two PVF_2–camphor compounds. From the polymer fraction related to the maximum of the melting enthalpy ($W_{PVF2} = 0.44 \pm 0.02$) associated with this thermal event, stoichiometry of compound C_1 can be estimated to be around *1 camphor*

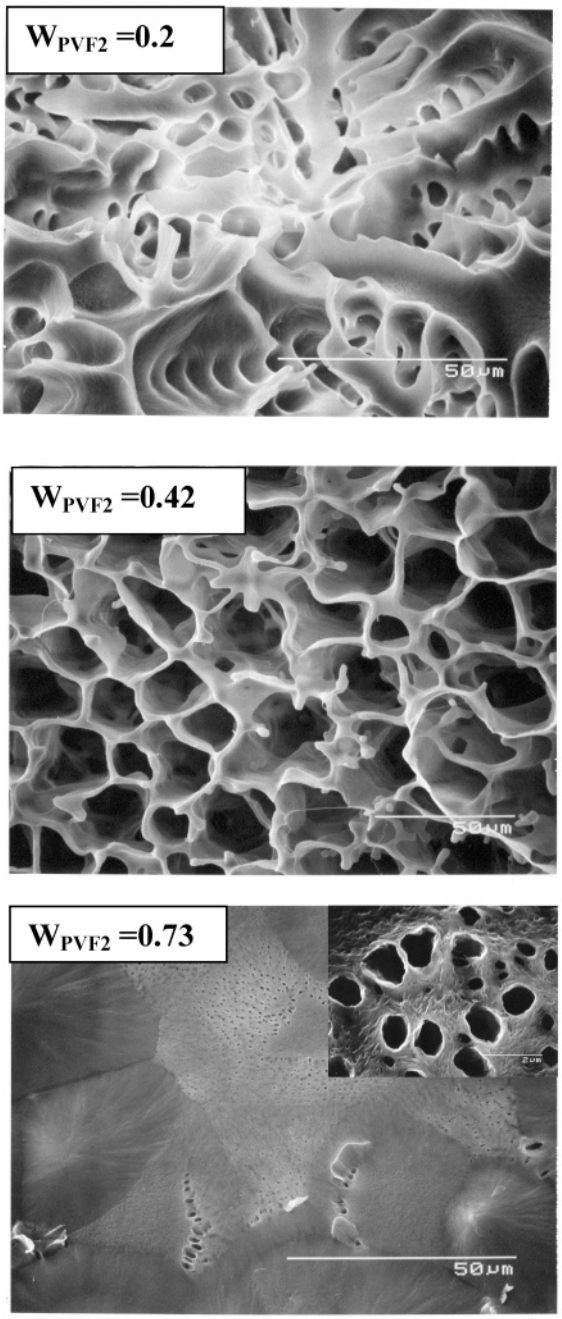

Figure 5. SEM picture of PVF_2−camphor system after the removal of camphor at indicated weight fraction of PVF_2.

*molecule for 2 monomer*s. Stoichiometry of compounds C_2 can be estimated from the polymer fraction, where melting enthalpy of compound C_1 becomes zero, namely, $W_{PVF2} = 0.64 \pm 0.02$, which eventually yields *1 camphor molecule for 4 monomers*. Compounds C_1 and C_2 are of the incongruently melting type.[15]

(ii) The nonvariant event at T = 142 °C is most probably a *metatectic* transition. This type of transition is observed when two crystalline forms exist for a pure compound. The metatectic composition is given through the melting enthalpy of solid-phase S_{P1} becoming zero, namely, at $W_{PVF2} = 0.52 \pm 0.02$. As has been discussed above, the thickening process of PVF_2 lamellae, which gives rise to two endotherms, is equivalent to the existence of two crystalline forms. At this temperature, compound C_2 transforms into a solid-phase S_{P2}, which is a mixture of thick PVF_2 crystal and camphor molecules. Here, camphor is likely to be located in the amorphous domains located between lamellae.

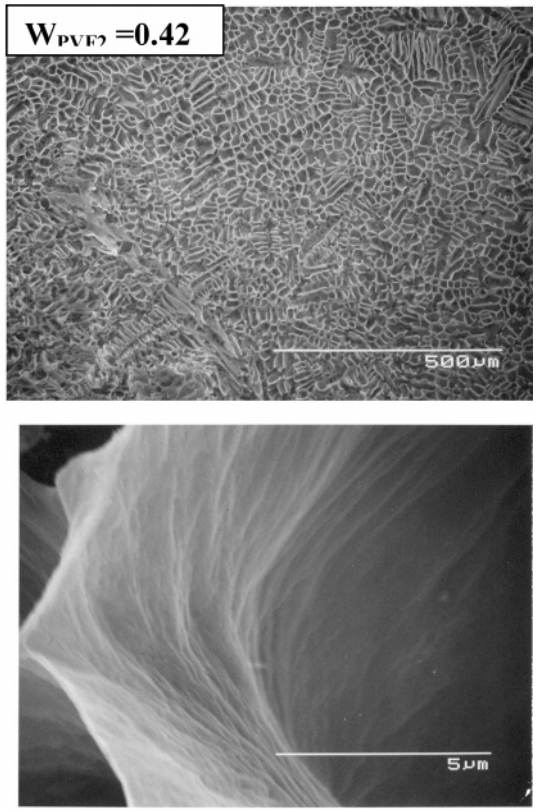

Figure 6. SEM picture of PVF_2−camphor system after the removal of camphor ($W_{PVF2} = 0.42$) at different magnification.

(iii) The nonvariant event at T = 145°C is most probably a eutectic transition, where solid-phase S_{P2} gives a polymer solution, while a solid solution, S_{cp}, remains. The latter consists mainly of camphor molecules wherein PVF_2 molecules are embedded. From the phase diagram, nothing can be said about its molecular structure. The eutectic polymer fraction is given, both through the melting enthalpy of solid-phase S_{cp} and that of solid-phase S_{P2}, becoming zero, namely, at $W_{PVF2} = 0.45 \pm 0.05$. As will be discussed below, this solid solution consists of camphor molecules and PVF_2 chains.

Morphology and Texture. Optical microscopy gives a clear insight into the textures occurring as a function of temperature. For a polymer fraction of $W_{PVF2} = 0.15$, one observes at room temperature a mosaic-like texture with fragmented domains of sizes above 100 μm wherein crosses are visible (Figure 3). This suggests some mechanism of self-epitaxy. At this temperature, one is dealing with a mixture $S_{cp} + C_1$ according to the temperature−concentration phase diagram. On heating at 140 °C, the texture changes drastically. Again, a mosaic-like texture shows up, but with domains of smaller size, the crosses have vanished. At this temperature, the $T-C$ phase diagram indicates a mixture of $S_{cp} + C_2$. This would mean that the transformation of C_1 into C_2 involves major morphological changes. At 160 °C, changes are still more drastic. Large domains with conspicuous digitation features appear. Here, the $T-C$ phase diagram indicates a mixture of liquid + S_{cp}, where the liquid is a concentration solution of camphor and PVF_2, and the solid S_{cp} phase contains essentially camphor molecules. Most probably, the liquid phase is responsible for the digitations. Note that none of the

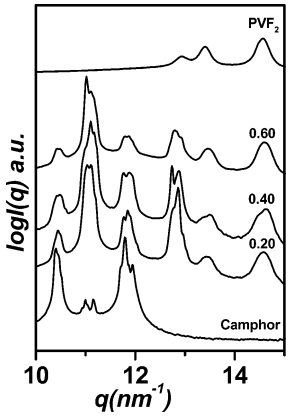

Figure 7. Room temperature (20 °C) Time-resolved X-ray scattering of PVF_2−camphor system at indicated weight fraction of PVF_2.

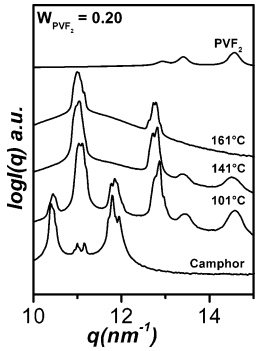

Figure 8. Time-resolved X-ray patterns of PVF_2−camphor system ($W_{PVF2} = 0.20$) at indicated temperatures.

features seen for $W_{PVF2} = 0.15$ pertain to the pure components.

Similar morphological changes are seen at $W_{PVF2} = 0.6$ (Figure 4), although crosses are no longer seen at $T = 20$ °C. At 140 °C, the overall texture is probably the same as with $W_{PVF2} = 0.15$, yet the mosaicity is tinier. At 160 °C, spherulites appear that can be most certainly attributed to semicrystalline PVF_2 as indicated by the phase diagram.

Scanning electronic micrographs shown in Figures 5 and 6 in the concentration range where the phase diagram indicates the existence of a compound and a solid solution of camphor, the morphology after camphor removal is tubular, with hollows to about 10−20 μm wide ($W_{PVF2} = 0.2$ and $W_{PVF2} = 0.42$). These are probably the features seen at 140°C, where compound C_1 has transformed into compound C_2. The network structure, together with reversible first-order phase transition (Figure 1), clearly indicates thermoreversible gel formation at these compositions.[22] At a polymer fraction $W_{PVF2} = 0.73$, for which one expects a mixture of compound C_2 and a solid PVF_2 phase, one does observe spherulites and a swiss-cheese like phase (see magnification in inset of Figure 5), the latter certainly corresponding to C_2. In the case of $W_{PVF2} = 0.42$, further magnification of the tubular structures reveals a lamellar morphology where lamellae are about 20 nm thick (Figure 6).

Time-Resolved X-ray Diffraction. The crystalline structure of the different phases has been studied by X-ray diffraction by time-resolved experiments at increasing temperature with the same rate as used for DSC experiments, namely, 2°C/min. The different polymer fractions studied, namely, $W_{PVF2} = 0.2$, 0.4, and 0.6,

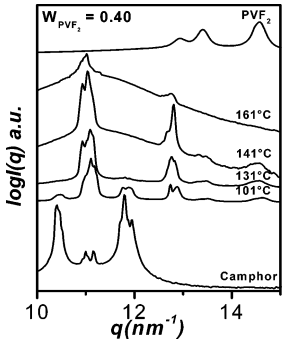

Figure 9. Time-resolved X-ray patterns of PVF_2−camphor system ($W_{PVF2} = 0.40$) at indicated temperatures.

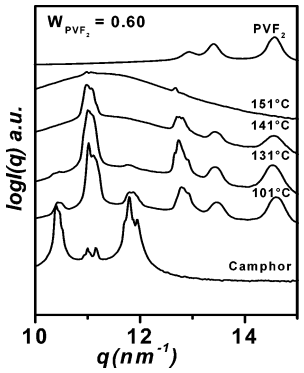

Figure 10. Time-resolved X-ray patterns of PVF_2−camphor system ($W_{PVF2} = 0.60$) at indicated temperatures.

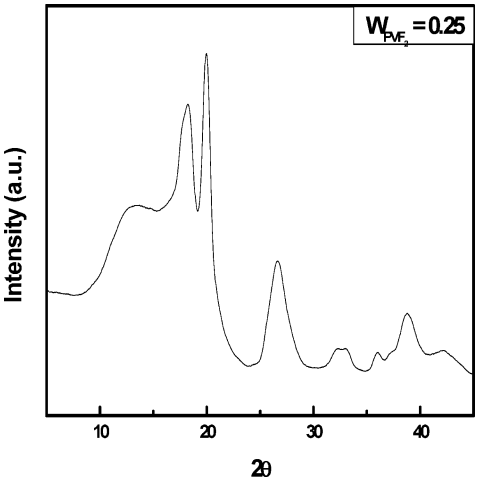

Figure 11. WAXS pattern of PVF_2−camphor system ($W_{PVF2} = 0.25$) after evaporation of camphor.

have been chosen on the basis of the outcomes of the temperature−concentration phase diagram.

In Figure 7 are drawn the diffraction patterns for these three polymer fractions as recorded at room temperature, together with those of pure camphor and of pure PVF_2. In all the diffraction patterns presented herein, the logarithm of the diffracted intensity is plotted as a function of the transfer momentum $q = 4\pi/\lambda \sin(\theta/2)$ (λ = wavelength and θ = diffraction angle). Two series of diffraction peaks centered around $q = 11$ nm^{-1} and $q = 12.8$ nm^{-1} are observed that are otherwise very weak for pure camphor and absent for pure PVF_2. These peaks are a clear indication that PVF_2−camphor compounds are present in the system, a conclusion in agreement with the outcomes from the temperature−concentration phase diagram. Peaks centered around $q = 10.4$ nm^{-1}, and $q = 11.8$ nm^{-1} may offhand suggest

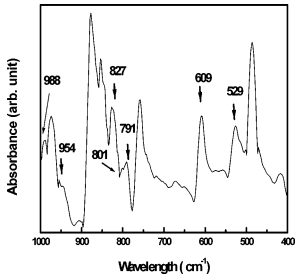

Figure 12. Camphor-subtracted FTIR spectrum of PVF_2−camphor system ($W_{PVF2} = 0.25$).

that free camphor is present. However, diffraction patterns obtained by increasing temperature, shown in Figures 8−10, do not confirm this point. As a matter of fact, these series of peaks vanish at 130 °C, which is well below the melting point of pure camphor. In light of the temperature−concentration phase diagram, we suspect that these peaks are actually related to compound C_1, as they disappear at the temperature where C_1 is said to transform into C_2, while those centered around $q = 11$ nm^{-1} and $q = 12.8$ nm^{-1} would be due both to compound C_2 and to the solid solution S_{cp}. As a matter of fact, for $W_{PVF2} = 0.2$, only those peaks are visible at $T = 161$ °C, for which temperature the phase diagram predicts the existence of a liquid phase and of the solid-phase S_{cp}. For $W_{PVF2} = 0.6$, these series of peaks are seen up to $T = 151$ °C. Clearly, a deeper study of the diffraction pattern will be needed to sort out the assignment of the different peaks, something which is beyond the scope of the present paper. Yet we may venture to put forward an explanation on the basis of inclusion compounds.[21] If polymer stems replace chains of camphor molecules in the camphor crystalline lattice, two cases may occur: (i) these stems are randomly dispersed so that a solid solution is produced, and (ii) these stems are regularly disposed, which corresponds

Table 1. WAXS Data of PVF_2−Camphor Dried Gel [d_{hkl} Calculated for α Phase of PVF_2 with $a = 5.02$ A°, $b = 9.63$ A°, and $c = 4.62$ A°], I^0_{hkl} = Observed Intensity

hkl	(d_{hkl}) calculated (A°)	(d_{hkl}) observed (A°)	I^0_{hkl}/I^0_{110} melt crystal	PVF_2 camphor gel $W_{PVF2} = 0.25$ I^0_{hkl}/I^0_{110}
100	5.00	4.99	0.68	0.77
020	4.81	4.82	0.92	0.82
110	4.44	4.43	1.00	1.00
021/101	3.33	3.35	0.48	0.48
121	2.79	2.76	0.24	0.292
130	2.7	2.71	0.25	0.30
200	2.49	2.5	0.24	0.29
	2.40	2.40	0.23	0.29
131	2.33	2.32	0.32	0.37
211/041	2.14	2.14	0.23	0.29

to the case of a compound. Under these conditions, the diffraction patterns of the compound and of the solid solution can be very similar.

The structure of a dried system has been determined from WAXS patterns and FTIR spectroscopy. A representative WAXS pattern of the PVF_2 dried system is shown in Figure 11. From the figure, it is evident that the WAXS pattern corresponds to that of α-polymorph of PVF_2.[23−26] In Table 1, the d_{hkl} values and intensity ratio (I^0_{hkl}/I^0_{110}) of dried gels are compared with those of the melt-crystallized samples. It is clear from the table that intensity ratio values of the dried gels do not exactly tally with those of the melt crystal.[24,25] It indicates that, although the d spacings remain the same, the atomic positions of the statistical up and down arrangement of the chains may be somewhat changed. The atomic coordinates in the unit cell are disturbed, which may be due to the occurrence of polymer−solvent complexation.

In Figure 12, the camphor-subtracted FT-IR spectra of PVF_2−camphor system at $W_{PVF2} = 0.23$ is presented. It is clear from the spectra that there are peaks at 801,

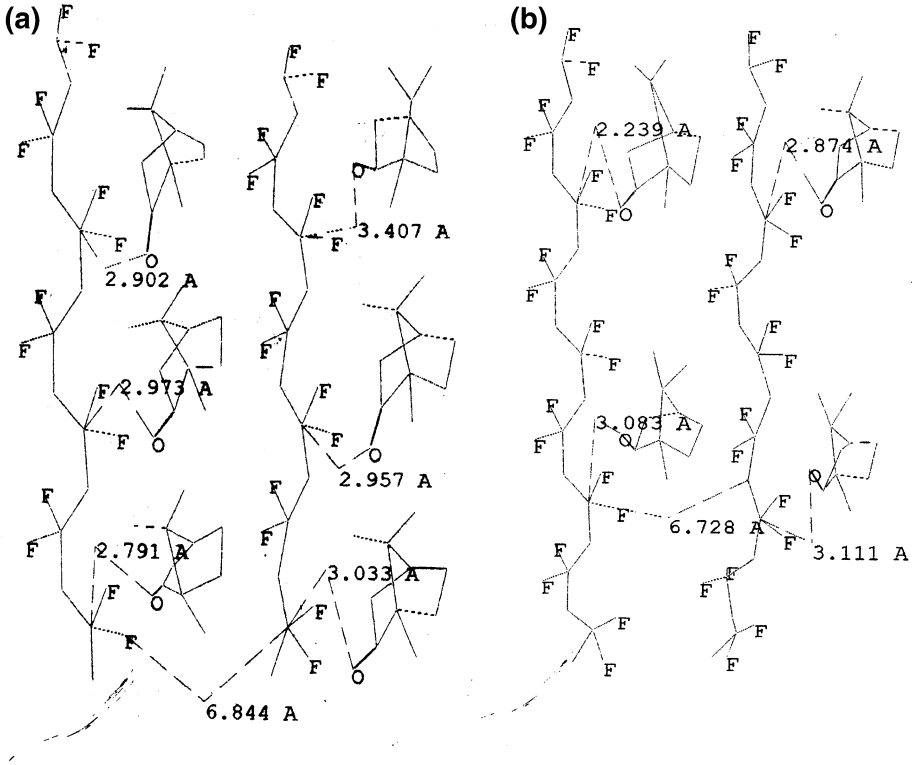

Figure 13. Molecular models of PVF_2(α-polymorph)−camphor complexes obtained from energy minimization through MMX program (a) C_1 (PVF_2 monomer unit: camphor = 2:1) (b) C_2 (PVF_2 monomer unit: camphor = 4:1).

609, and 529 cm^{-1} characteristic of α-polymorph of PVF_2.[27−29] Thus, FTIR spectra confirm the presence of an α-polymorph in the undried state, and no change in the polymorphic structure of PVF_2 occurred during the removal of camphor, as the X-ray pattern of dried PVF_2 gel also exhibited an α-polymorphic structure. Some new peaks at frequencies of 988, 954, 827, and 791 cm^{-1} appeared that may correspond to those for the polymer−solvent complexation.[7,14]

Molecular Modeling. An approximate idea of the model structure of PVF_2−camphor complexes may be done by using molecular mechanics calculations with the help of the MMX method. Camphor molecules are placed by the side of PVF_2 chains (α phase), such that ⟩C═O group of camphor faces ⟩CF_2 group of PVF_2, as there is some dipolar interaction between these two groups.[9,10] The ratio of camphor molecules and PVF_2 monomeric units is 1:2 in Figure 13a and 1:4 in Figure 13b. The whole structure was then energetically minimized using the MMX program, and the distance between the carbon atom of ⟩CF_2 group and oxygen atom of ⟩C═O group is queried. The van der Waals radius of ⟩CF_2 group is 2.25 Å and that of oxygen is 1.4 Å, yielding the distance of interatomic contact to be 3.65 Å.[7,30] In all the cases, the queried distances are less than 3.65 Å, primarily supporting the PVF_2−camphor compound formation. The distance between the PVF_2 strands is about 6.7−6.8 Å, i.e., pores of diameter 6.8 Å may be obtained after careful removal of camphor from the gel. Such subnanometer-sized pores are difficult to observe in a scanning electron microscope, and to measure these pores, sophisticated nitrogen gas porosimetry with nonlinear density functional theory (NLDFT) technique is needed. Thus, in these samples, the presence of macro, meso, and micropores is suggested and will be addressed in our forthcoming publication.

Conclusion

PVF_2−camphor systems exhibit interesting porous morphology after camphor removal, which changes with PVF_2 concentration. WAXS and FTIR results suggest the formation of an α-polymorph of PVF_2 in the gels. Atomic coordinates of an α-polymorph crystal of PVF_2 may be somewhat changed for the polymer−solvent complex formation. A complex temperature−concentration phase diagram is observed, which suggests the formation of two incongruently melting polymer−camphor compounds, a eutectic transition, and a metatectic transition. Time-resolved X-ray diffraction experiments provide further evidence of the occurrence of polymer−solvent complex C_1 and its transformation into compound C_2 with increasing temperature. The texture of the blend changes with increasing temperature due to the transition from C_1 to C_2 and then to the solid solution phase. With increasing PVF_2 concentration, the texture has changed but the features with increasing temperature remains almost the same as earlier. SEM pictures at low concentration yields a tubular structure, but at a higher concentration (W_{PVF2} = 0.73), both spherulites and a swiss-cheese like phase are observed. From these tubular structures, porous material possessing filtering properties can be prepared.

Acknowledgment. S. Malik and D. Dasgupta are indebted to IFCPAR (Indo-French Center for the Promotion of Advanced Research) for a grant-in-aid for a postdoctoral position (ICS, Strasbourg) and for a Ph.D. thesis (IACS, Kolkata), respectively. The authors are indebted to IFCPAR for research grant No. 2808-2. The camera equipping the optical microscope together with the image processing software were financed through this grant.

References and Notes

(1) *Reversible Polymeric Gels and Related Systems*; Russo, P. S. Ed.; American Chemical Society: Washington DC, 1987.
(2) Guenet, J. M. *Thermoreversible Gelation of Polymers and Biopolymers*; Academic Press: New York, 1992.
(3) NiJenhuis, K. te. *Adv. Polym. Sci,* **1997**, *130*, 1.
(4) Lovinger, A. J. In *Development in Crystalline Polymers, 1*; Basset, D. C. Ed.; Elsevier Applied Science: London 1981; p 195.
(5) Mal, S.; Maiti, P.; Nandi, A. K. *Macromolecules* **1995**, *28*, 2371.
(6) Cho, J. W.; Song, H. Y.; Kim, S. Y. *Polymer* **1993**, *34*, 1024.
(7) Dikshit, A. K.; Nandi, A. K. *Macromolecules* **2000**, *33*, 2616.
(8) Milano, G.; Venditto, V.; Guerra, G.; Cavallo, L.; Caimbelli, P.; Sannino, D. *Chem Mater*. **2001**, *13*, 1506.
(9) Roerdink, E.; Challa, G. *Polymer* **1980**, *21*, 509.
(10) Belke, R. E.; Cabasso, I. *Polymer* **1988**, *29*, 1831.
(11) Jana, T.; Nandi, A. K. *Langmuir* **2000**, *16*, 3141; Jana, T.; Nandi, A. K. *Langmuir* **2001**, *17*, 3607.
(12) Vikki, T.; Ruokolainen, J.; Ikkala, O. T.; Passiniemi, P.; Isotalo, H.; Torkkeli, M.; Serimoa, R. *Macromolecules* **1997**, *30*, 4064.
(13) Rahman, M. H.; Malik, S.; Nandi, A. K. *Macromol. Chem. Phys*. **2003**, *204*, 1765.
(14) Dikshit, A. K.; Nandi, A. K. *Macromolecules* **1998**, *31*, 8886.
(15) Guenet, J. M.; McKenna, G. B. *Macromolecules* **1988**, *21*, 1752.
(16) Spevacek, J.; Suchopanek, M. *Macromolecules* **1998**, *31*, 703.
(17) Gajewski, K. E.; Gilberr M. H. In *Advances in Molecular Modelling*; Liotta D. Ed.; JAI Press: Greenerick. CT, 1990; Vol. 2.
(18) Nagumo, T.; Matsuo, T.; Suga, H. *Thermochim. Acta*, **1989**, *139, 121*.
(19) Prest, W. M. Jr.; Luca, D. J. *J. Appl. Phys*. **1975**, *46*, 4136.
(20) Prest, W. M. Jr.; Luca, D. J. *Bull. Am. Phys. Soc*. **1974**, *19*, 217.
(21) Chenite, A.; Brisse, F. *Macromolecules* **1991**, *24*, 2221.
(22) Daniel, C.; Dammer, C.; Guenet J. M. *Polym. Commun*. **1994**, *35*, 4243.
(23) Lando, J. B.; Doll, W. W. *J. Macromol Sci., Phys*. **1968**, *2*, 205.
(24) Hasegawa, R.; Takahashi Y.; Chatani, Y. *Polym. J*. **1972**, *3*, 600.
(25) Bachmann, M. A.; Lando, J. B. *Macromolecules* **1981**, *14*, 40.
(26) Datta, J.; Nandi, A. K. *Polymer* **1997**, *38*, 2719.
(27) Cortill, G.; Zebri, G. *Spectrochim. Acta, Part A* **1967**, *23*, 2218.
(28) Tashiro, K.; Kobayashi, M. *Phase Transitions* **1989**, *18*, 213.
(29) Kobayashi, M.; Tashiro, K.; Tadokaro, H. *Macromolecules* **1975**, *8*, 158.
(30) Pauling, L. *The Nature of Chemical Bond and the Structure of Molecules and Crystals,* 3rd ed.; Cornell University Press: Ithaca, NY, 1960; p 227.

MA050582A